Capacity Improvement with NOMA-CI Precoding for MU-MISO Downlink Systems

Yanfei Lu, Qing Li, Qinghe Gao, Yingzhen Wu, Yan Huo, Tao Jing
School of Electronics and Information Engineering, Beijing Jiaotong University, Beijing, China
E-mail: {yflu,22120081,qhgao,yingzhenwu,yhuo,tjing}@bjtu.edu.cn

***Abstract*—In the communication process of the Internet of Things (IoT), non-orthogonal multiple access (NOMA) technology is usually used to improve spectrum efficiency and system capacity. However, due to the wide application of multimedia in the IoT, the high amount of data generated puts a higher demand on the system capacity. Each targeted user in a NOMA group uses successive interference cancellation (SIC) to decode useful information where the signals from other users are usually taken as interference, which hinders the improvement of the system capacity. In addition, the transmit power distribution between groups does not consider edge users, which affects the fairness of users. To solve above problems, we propose to combine the constructive interference (CI) precoding with NOMA by making the interference between users constructive for each NOMA user. Specifically, the NOMA-CI precoding is dedicatedly designed to improve the system capacity and a proportional power distribution scheme between NOMA groups is deployed to improve the capacity for edge users. We conduct extensive simulation experiments by comparing with existing schemes under different modulation methods, which demonstrate our scheme can improve the system capacity than the NOMA scheme by about 60% and achieve significant increase of the edge user capacity, enhancing the system fairness.**

***Index terms*—** NOMA, constructive interference, precoding, capacity improvement, fairness enhancement.

I. Introduction

Multimedia devices in the Internet of Things (IoT) are connected to the Internet by wired or wireless means, forming a convenient and efficient data transmission channel to achieve efficient communication of information, so the data is showing explosive growth, and it is urgent to improve the capability and efficiency of the communication system [1], [2]. Non-orthogonal multiple access (NOMA) is one of the promising multiple access technologies. Traditional NOMA uses appropriate power allocation to enable multiple users to use the same resource and applies successive interference cancellation (SIC) technology at the receiver to distinguish different users [3]. At present, many scholars have conducted in-depth research on power distribution to improve the capacity for edge users: [4] proposed fixed power allocation algorithm that controls power allocation through the channel gain ratio; [5] proposed iterative power allocation algorithm based on the greedy algorithm; [6] proposed full space search power allocation algorithm based on the exhaustive solution of users. In addition, studies on NOMA have focused mainly on user clustering to improve system performance [7]. However, in NOMA networks, each user employs SIC methods to decode useful information and treats other user information as interference, which greatly affects the increase of system capacity.

Information from other users is not utilized in multi-user NOMA networks, which creates opportunities for constructive interference (CI)-based technologies. CI precoding can transform harmful multi-user interference (MUI) into beneficial signals, significantly improving the performance of multi-user communication systems [8]. The existing literature [9] has proved the advantages of this scheme in multi-user multiple-input single-output (MU-MISO) systems, which can effectively reduce the symbol-error-rate (SER) of the system. By properly designed precoding and precoding methods, the desired data symbols at the receiver are guided into the construction domain of the transmitted symbols, which can simplify the demodulation process at the receiver and improve the quality of the received signal. Domestic and foreign research hotspots on CI mainly focus on multi-user clustering [8], physical layer security [10], etc. However, system performance improvement has never been considered in the coding process, how to make full use of CI and further improve system capacity is an urgent problem to be solved.

In this paper, we propose NOMA-CI precoding based on CI and NOMA for MU-MISO downlink systems. Specifically, a suitable precoding matrix is designed on the basis of making full use of the interference between multiple users and considering the fairness of users, so that the receiver can get the expected received signal without complex demodulation after removing the high-power signal. And a proportional power distribution scheme is proposed to improve the capacity for edge users.

The main contributions of the paper are summarized as follows.

- We propose a novel NOMA-CI precoding that combines power allocation with constructive interference precoding to make the received signal constructive to NOMA users.
- We propose a proportional inter-group power distribution scheme to improve the capacity for edge users.
- We use Lagrange and Karush-Kuhn-Tucke (KKT) to solve the optimization problem and get closed-form solution of precoding matrix.

The rest of the paper is organized as follows. The preliminaries are reviewed in Section II, including the basic concepts of CI and NOMA. The system model and problem formulation are presented in Section III, including the system model, user

979-8-3503-7099-7/24/$31.00 ©2024 IEEE

grouping, power distribution and optimization problem. Then we solve the optimization problem in Section IV. We show the simulation results in Section V and draw conclusions in Section VI. Section VII is the item number.

II. PRELIMINARIES

A. Non-Orthogonal Multiple Access

In order to increase system capacity, NOMA achieves multi-user multiplexing in the power domain. In multi-user downlinks, the transmitter superpositions the user signals by power allocation, where the user with poor channel gain is allocated more power, and then the correct demodulation is achieved by SIC technique at the receiver [11]. Fig. 1 shows the process of SIC elimination at the receiver of two users. The information rate of user 1 is

$$R_1 = \log_2(1 + \frac{P_1 \mid \boldsymbol{h}_1 \mid^2}{P_2 \mid \boldsymbol{h}_1 \mid^2 + n_0}), \tag{1}$$

the information rate of user 2 is

$$R_2 = \log_2(1 + \frac{P_2 \mid \boldsymbol{h}_2 \mid^2}{n_0}), \tag{2}$$

where P_1 is the power allocated to user 1, P_2 is the power allocated to user 2, s_1, s_2 are the signals sent by the base station (BS) to user 1 and user 2, $\mid s_1 \mid^2 = \mid s_2 \mid^2 = 1$, n_0 is the noise power at the receiver with the bandwidth of 1Hz, and $\boldsymbol{h}_1, \boldsymbol{h}_2$ are the channel coefficients.

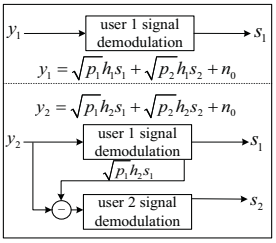

Fig. 1. Demodulation diagram of two-user receiver.

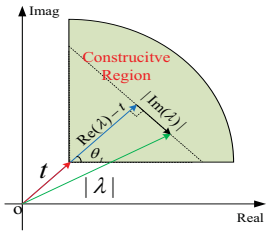

Fig. 2. Non-strict phase rotation.

B. Constructive Interference

With the help of symbol level precoding, CI precoding abandons the old idea of interference cancellation. By rotating the phase of the transmitted data, the interference signal is aligned with the signal of interest at each receiver, so that the generated symbols are far away from the original decision threshold of the constellation diagram and fall into the construction region [12]. To more clearly demonstrate the concept of construction interference, we present an example of a non-strict phase rotation in Fig. 2. Assume the BS with N_t transmit antennas is communicating with K_t single-antenna users and represent the received noiseless signal of user k as y_k,

$$y_k = \boldsymbol{h}_k \boldsymbol{W} \boldsymbol{s} = \lambda s_k, \tag{3}$$

where $\boldsymbol{h}_k \in \mathcal{C}^{1 \times N_t}$ represents the channel vector, $\boldsymbol{W} \in \mathcal{C}^{N_t \times K_t}$ denotes the precoding matrix, $\boldsymbol{s} \in \mathcal{C}^{K_t \times 1}$ is the symbol vector, and λ is a scaling factor of the construction domain.

The construction region of s_k is a green sector with infinite radius at angle $2\theta_t$ in the Fig. 2. For the multiple phase shift keying (MPSK) modulation, $\theta_t = \frac{\pi}{M}$. The distance between the construction region and the decision boundary depends on $t = \sqrt{\Gamma \sigma^2}$, where Γ denotes the signal-to-noise ratio (SNR) requirement for user, σ^2 is the noise power at the user. Using symbolic information and channel state information (CSI), the CI-based precoding ensures the noiseless signal received is located in the construction region of each user's expected symbol. The construction region of s_k can be defined by the following inequality

$$\mid \Im(\lambda) \mid \leq \tan\theta_t [\Re(\lambda) - t], \tag{4}$$

where $\Re(\lambda)$ represents the real part of λ, $\Im(\lambda)$ represents the imaginary part of λ.

III. SYSTEM MODEL AND PROBLEM FORMULATION

A. System Model

In this paper, we consider a downlink MU-MISO system, where a BS equipped with N transmit antennas serves K single-antenna users simultaneously over the Rayleigh fading channel. The symbol vector transmitted at the time slot is denoted as $\boldsymbol{s} = \{s_1, s_2, \ldots, s_K\}^T$ and $\mid s_k \mid^2 = 1$, $k \in [1, K]$, where each symbol is independently selected from MPSK constellations.

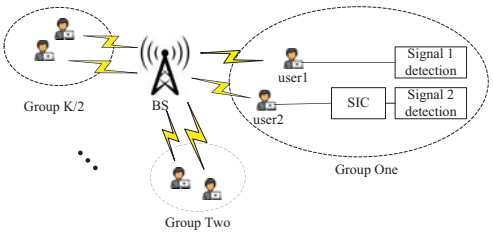

Fig. 3. System model.

As shown in Fig. 3, the link groups multiple users in pairs according to the channel gains. The sub-channel transmission still adopts orthogonal frequency division multiple access (OFDMA) technology, so different groups are orthogonal to each other without interference. However, users in the same group do not have orthogonal transmission, and the channel conditions of user2 are better than user1. User1 in the g-th group can directly decode the correct information. User2 uses the SIC technique to eliminate high-power signals and decodes directly for the correct information.

B. Grouping Strategy

Sort the user channel gains and divide all users into core, intermediate, and edge users. SIC is suitable for user grouping with large channel gain differences, so our algorithm can improve the system performance as much as possible while maintaining complexity. Specifically, first we take the middle

value of the sorted channel gain as the threshold, and then we divide the user set into two clusters, finally, one user from the strong user cluster and the weak user cluster are assigned to the same group in order, as illustrated in Fig. 4.

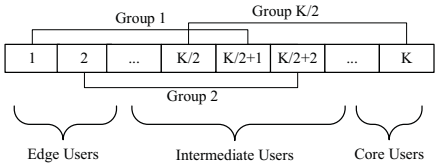

Fig. 4. User matching algorithm.

C. Inter-group Power Distribution

Existing inter-group power distribution methods are average power distribution and waterfilling distribution, which will reduce edge users' capacity and affect users' fairness. Therefore, this paper allocates more power to the group with smaller channel gain. In addition, to ensure the simplicity of calculation, we employ a proportional power distribution scheme where fixed power factors are allocated to different groups to complete the power allocation. Specifically, the allocation strategy can be expressed as

$$p_1 = a * power, \tag{5a}$$

$$p_{g+1} = a * p_g \quad \forall g \in \{1, ..., K/2 - 1\}, \tag{5b}$$

where a represents the fixed power distribution factor and $0 < a < 1$, $power$ is the transmitting power of the BS and p_g denotes the transmit power of the g-th group. When the number of users is large, we can get that $a = 0.5$ according to the arithmetic series summation formula.

D. Intra-group Symbol-Level Precoding

The signals received by the first user and the second user in the g-th group can be written as

$$y_{g,1} = \boldsymbol{h}_{g,1}^T \boldsymbol{W}_g(s_{g,1} + bs_{g,2}) + n_{g,1}, \tag{6a}$$

$$y_{g,2} = \boldsymbol{h}_{g,2}^T \boldsymbol{W}_g bs_{g,2} + n_{g,2}, \tag{6b}$$

where $\boldsymbol{h}_{g,1}$, $\boldsymbol{h}_{g,2} \in \mathcal{C}^N$ represent the channel vectors between the BS and users within the g-th group, in this paper we assume perfect CSI is known at the BS. $\boldsymbol{W}_g \in \mathcal{C}^N$ stands for the precoding matrix of the g-th group, b denotes the power distribution factor within the g-th group and $0 < b < 1$. $n_{g,1}, n_{g,2} \sim \mathcal{CN}(0, \frac{2N_0B}{K})$ are the additive white Gaussian noise (AWGN), N_0 is this system's AWGN power spectral density, and B represents the total system bandwidth.

In order to make full use of the information of other users in the traditional NOMA scheme, this paper optimizes the symbolic information of all users with a precoder, enabling the conversion of the intra-group MUI to CI. Considering user fairness, the max-min problem for designing $\boldsymbol{W}_g$ can be formulated as

$$\mathcal{P}1: \max_{\boldsymbol{W}_g, t, t_1, t_2} \quad t \tag{7a}$$

$$\text{s.t.} \quad \boldsymbol{h}_{g,1}^T \boldsymbol{W}_g(s_{g,1} + bs_{g,2}) = \lambda_1 s_{g,1} \tag{7b}$$

$$\boldsymbol{h}_{g,2}^T \boldsymbol{W}_g(bs_{g,2}) = \lambda_2 s_{g,2} \tag{7c}$$

$$|\, \Im(\lambda_1) \,| \leq \tan\theta_t [\Re(\lambda_1) - t_1] \tag{7d}$$

$$|\, \Im(\lambda_2) \,| \leq \tan\theta_t [\Re(\lambda_2) - t_2] \tag{7e}$$

$$\| \boldsymbol{W}_g(s_{g,1} + bs_{g,2}) \|_2^2 \leq p_g \tag{7f}$$

$$t, t_1, t_2 \geq 0 \tag{7g}$$

$$t \leq t_1 \tag{7h}$$

$$t \leq t_2 \tag{7i}$$

where t_1, t_2 are positively correlated with SNR of $s_{g,1}$ and $s_{g,2}$ respectively. We consider the case of quadrature phase shift keying (QPSK) modulation, so the threshold angle $\theta_t = \frac{\pi}{4}$. (7b), (7c), (7d), (7e) ensure that noiseless signal received at each user is located within the construction area of transmitted symbol. The information rates of users in the g-th group are

$$R_{g,1} = \frac{4B}{K} \log_2(1 + \frac{Kt_1^2}{2N_0B}), \tag{8a}$$

$$R_{g,2} = \frac{4B}{K} \log_2(1 + \frac{Kt_2^2}{2N_0B}). \tag{8b}$$

We set b to iterate from 0.1 to 0.9 with an iteration step of 0.1, and choose the solution of the optimization problem that maximizes $R_{g,1} + R_{g,2}$ as the optimal solution, so the total system capacity is

$$C = \sum_{g=1}^{K/2} R_{g,1} + R_{g,2}. \tag{9}$$

The optimization problem is convex and we will solve it in detail in the next section.

IV. SIMPLIFIED ALGORITHM FOR MAX-MIN PROBLEM

In this section, we solve the above max-min problem. First, we simplify the optimization problem, transform $\mathcal{P}_1$ into a standard minimization problem, expressed as

$$\mathcal{P}2: \min_{\boldsymbol{W}_g, t, t_1, t_2} \quad -t \tag{10a}$$

$$\text{s.t.} \quad \boldsymbol{h}_{g,1}^T \boldsymbol{W}_g(s_{g,1} + bs_{g,2}) - \lambda_1 s_{g,1} = 0 \tag{10b}$$

$$\boldsymbol{h}_{g,2}^T \boldsymbol{W}_g(bs_{g,2}) - \lambda_2 s_{g,2} = 0 \tag{10c}$$

$$\Im(\lambda_1) - [\Re(\lambda_1) - t_1] \leq 0 \tag{10d}$$

$$-\Im(\lambda_1) - [\Re(\lambda_1) - t_1] \leq 0 \tag{10e}$$

$$\Im(\lambda_2) - [\Re(\lambda_2) - t_2] \leq 0 \tag{10f}$$

$$-\Im(\lambda_2) - [\Re(\lambda_2) - t_2] \leq 0 \tag{10g}$$

$$|\, s_{g,1} + bs_{g,2} \,|^2 \, \boldsymbol{W}_g^H \boldsymbol{W}_g - p_g \leq 0 \tag{10h}$$

$$-t, -t_1, -t_2 \leq 0 \tag{10i}$$

$$t - t_1 \leq 0 \tag{10j}$$

$$t - t_2 \leq 0 \tag{10k}$$

In the following we analyze $\mathcal{P}2$ with Lagrangian and KKT conditions. The Lagrangian of $\mathcal{P}2$ is expressed as

$$\begin{aligned}\mathcal{L}(\boldsymbol{W}_g, t, t_1, t_2) &= -t + v_1[\boldsymbol{h}_{g,1}^T \boldsymbol{W}_g(s_{g,1} + bs_{g,2}) - \lambda_1 \\ & s_{g,1}] + v_2[\boldsymbol{h}_{g,2}^T \boldsymbol{W}_g(bs_{g,2}) - \lambda_1 s_{g,1}] + \mu_1[\Im(\lambda_1) - \\ & (\Re(\lambda_1) - t_1)] + \mu_2[-\Im(\lambda_1) - (\Re(\lambda_1) - t_1)] + \mu_3 \\ & [\Im(\lambda_2) - (\Re(\lambda_2) - t_2)] + \mu_4[-\Im(\lambda_2) - (\Re(\lambda_2) \\ & - t_2)] + \mu_5(\mid s_{g,1} + bs_{g,2} \mid^2 \boldsymbol{W}_g^H \boldsymbol{W}_g - p_g) + \mu_6 \\ & (-t) + \mu_7(-t_1) + \mu_8(-t_2) + \mu_9(t - t_1) + \mu_{10}(t - t_3),\end{aligned} \tag{11}$$

where v_1,v_2,μ_i are the dual variables, and we have $\mu_i \geq 0$, $i \in [1, 10]$. Based on the Lagrangian in (11), the KKT conditions for optimality can be obtained as

$$\begin{aligned}\frac{\partial \mathcal{L}}{\partial \boldsymbol{W}_g} &= v_1 h_{g,1}^T(s_{g,1} + bs_{g,2}) + v_2 \boldsymbol{h}_{g,2}^T(bs_{g,2}) \\ &+ \mu_5 \mid s_{g,1} + bs_{g,2} \mid^2 \boldsymbol{W}_g^H = 0, \qquad (12a) \\ \mu_5(\mid s_{g,1} + bs_{g,2} \mid^2 \boldsymbol{W}_g^H \boldsymbol{W}_g &- p_g) = 0. \qquad (12b)\end{aligned}$$

Based on (12a), it is firstly obtained that $\mu_5 \neq 0$, and with the fact that $\mu_5 \geq 0$, we can further obtain $\mu_5 > 0$. Then, $\boldsymbol{W}_g$ can be expressed as

$$\boldsymbol{W}_g = \Lambda_1 \boldsymbol{h}_{g,1}^T(s_{g,1} + bs_{g,2}) + \Lambda_2 \boldsymbol{h}_{g,2}^T(bs_{g,2}), \tag{13}$$

by substituting (13) into (10b) and (10c), we can further obtain

$$\Lambda_1 = \frac{A_1\lambda_1 + A_2\lambda_2}{A_3}, \tag{14a}$$

$$\Lambda_2 = \frac{B_1\lambda_1 + B_2\lambda_2}{B_3}, \tag{14b}$$

where we note that

$$\begin{aligned}A_1 &= b \parallel h_{g,2}^T \parallel_2^2 s_{g,1}, \qquad (15a) \\ A_2 &= -h_{g,1}^T(h_{g,2}^T)^H(s_{g,1} + bs_{g,2}), \qquad (15b) \\ A_3 &= b \parallel h_{g,1}^T \parallel_2^2 \parallel h_{g,2}^T \parallel_2^2 \mid s_{g,1} + bs_{g,2} \mid^2 \\ &- bh_{g,2}^T(h_{g,1}^T)^H h_{g,1}^T(h_{g,2}^T)^H \mid s_{g,1} + bs_{g,2} \mid^2, \qquad (15c) \\ B_1 &= bs_{g,1}s_{g,2} - h_{g,2}^T(h_{g,1}^T)^H, \qquad (15d) \\ B_2 &= -s_{g,2}(s_{g,1} + bs_{g,2}) \parallel h_{g,1}^T \parallel_2^2, \qquad (15e) \\ B_3 &= b^2 h_{g,1}^T(h_{g,2}^T)^H h_{g,2}^T(h_{g,1}^T)^H(s_{g,1} + bs_{g,2}) \\ &- b^2 \parallel h_{g,1}^T \parallel_2^2 \parallel h_{g,2}^T \parallel_2^2 (s_{g,1} + bs_{g,2}), \qquad (15f)\end{aligned}$$

then $\boldsymbol{W}_g$ can be respectively rewritten in matrix closed-form as

$$\boldsymbol{W}_g = \boldsymbol{h}^H \boldsymbol{G} \boldsymbol{\lambda}, \tag{16}$$

where

$$\boldsymbol{h} = [\boldsymbol{h}_{g,1}^T, \boldsymbol{h}_{g,2}^T], \boldsymbol{\lambda} = [\lambda_1, \lambda_2]^T, \tag{17a}$$

$$\boldsymbol{G} = \begin{bmatrix} \frac{A_1}{A_3}(s_{g,1} + bs_{g,2})^H & \frac{A_2}{A_3}(s_{g,1} + bs_{g,2})^H \\ \frac{B_1}{B_3} bs_{g,2}^H & \frac{B_2}{B_3} bs_{g,2}^H \end{bmatrix}. \tag{17b}$$

With the fact that $\mu_5 > 0$, based on (12b) we can obtain that the power constraint is strictly active, which leads to

$$\mid s_{g,1} + bs_{g,2} \mid^2 \boldsymbol{W}_g^H \boldsymbol{W}_g - p_g = 0. \tag{18}$$

Substituting (16) into the (18), it is firstly obtained that

$$\boldsymbol{\lambda}^H \boldsymbol{J} \boldsymbol{\lambda} = p_g^o, \tag{19}$$

where we note

$$p_g^o = \frac{p_g}{\mid s_{g,1} + bs_{g,2} \mid^2}, \tag{20a}$$

$$\boldsymbol{J} = \boldsymbol{G}^H \boldsymbol{h} \boldsymbol{h}^H \boldsymbol{G}, \tag{20b}$$

and since the variables $\boldsymbol{\lambda}$ and $\boldsymbol{J}$ are complex, we need to decompose them to the real variables before settling the optimization problem. Let $\widehat{\boldsymbol{\lambda}} = [Re(\boldsymbol{\lambda}), Im(\boldsymbol{\lambda})]^T$,$\widehat{\boldsymbol{J}} = [Re(\boldsymbol{J}), -Im(\boldsymbol{J}); Im(\boldsymbol{J}), Re(\boldsymbol{J})]$. And in order to simplify the problem $\mathcal{P}2$, we define $\boldsymbol{r_1} = [t_1, t_2]^T$,$\boldsymbol{K_3} = [1, 1]^T$,

$\boldsymbol{K_1}$= $\begin{bmatrix} -1 & 0 & 1 & 0 \\ 0 & -1 & 0 & 1 \\ -1 & 0 & -1 & 0 \\ 0 & -1 & 0 & -1 \end{bmatrix}$, $\boldsymbol{K_2}$= $\begin{bmatrix} 1 & 0 \\ 0 & 1 \\ 1 & 0 \\ 0 & 1 \end{bmatrix}$. Thus, $\mathcal{P}2$ can be formulated as

$$\begin{aligned}\mathcal{P}3: \quad & \min_{\widehat{\boldsymbol{\lambda}}, t, \boldsymbol{r_1}} \quad -t \qquad (21a) \\ \text{s.t.} \quad & \widehat{\boldsymbol{\lambda}}^H \widehat{\boldsymbol{J}} \widehat{\boldsymbol{\lambda}} - p_g^o = 0 \qquad (21b) \\ & \boldsymbol{K_1} \widehat{\boldsymbol{\lambda}} + \boldsymbol{K_2} \boldsymbol{r}_1 <= \boldsymbol{0}_{4\times 1} \qquad (21c) \\ & \boldsymbol{K_3} t - \boldsymbol{r}_1 <= \boldsymbol{0}_{2\times 1} \qquad (21d) \\ & -t <= 0 \qquad (21e)\end{aligned}$$

The Lagrangian of $\mathcal{P}3$ is expressed as

$$\begin{aligned}\mathcal{L}(\widehat{\boldsymbol{\lambda}}, t, \boldsymbol{r}_1) = & -t + \alpha_0(\widehat{\boldsymbol{\lambda}}^H \widehat{\boldsymbol{J}} \widehat{\boldsymbol{\lambda}} - p_g^o) + \boldsymbol{\beta}_0^T(\boldsymbol{K_1} \widehat{\boldsymbol{\lambda}} + \boldsymbol{K_2} \boldsymbol{r}_1) \\ & + \boldsymbol{\beta}_1^T(\boldsymbol{K_3} t - \boldsymbol{r}_1) + \beta_2(-t).\end{aligned} \tag{22}$$

We express the KKT conditions optimality in the following with the non-zero dual variables $\alpha_0, \boldsymbol{\beta}_0, \boldsymbol{\beta}_1, \beta_2$

$$\frac{\partial \mathcal{L}}{\partial \widehat{\boldsymbol{\lambda}}} = 2\alpha_0 \widehat{\boldsymbol{J}} \widehat{\boldsymbol{\lambda}} + \boldsymbol{K_1}^T \boldsymbol{\beta}_0 = \boldsymbol{0}_{4\times 1}, \tag{23a}$$

$$\frac{\partial \mathcal{L}}{\partial \boldsymbol{r}_1} = \boldsymbol{K_2}^T \boldsymbol{\beta}_0 - \boldsymbol{\beta}_1 = \boldsymbol{0}_{2\times 1}, \tag{23b}$$

$$\frac{\partial \mathcal{L}}{\partial t} = -1 + \boldsymbol{K_3}^T \boldsymbol{\beta}_1 - \beta_2 = 0. \tag{23c}$$

Due to the fact that $\alpha_0 > 0$, we can obtain the closed-form solution of $\widehat{\boldsymbol{\lambda}}$ from (23a) as

$$\widehat{\boldsymbol{\lambda}} = \frac{\widehat{\boldsymbol{J}}^{-1} \boldsymbol{K_1}^T \boldsymbol{\beta}_0}{2\alpha_0}, \tag{24}$$

where we note that $\widehat{\boldsymbol{J}}$ is symmetric, so

$$\alpha_0 = \sqrt{\frac{\boldsymbol{\beta}_0^H \boldsymbol{L}^{-1} \boldsymbol{\beta}_0}{4p_g}}, \tag{25}$$

and we let

$$\boldsymbol{L}^{-1} = \boldsymbol{K_1} \widehat{\boldsymbol{J}}^{-1} \boldsymbol{K_1}^T. \tag{26}$$

Since $\mathcal{P}3$ is a convex problem, the strong duality holds as the Slater's condition is satisfied. To this end, the corresponding dual problem is given by

$$\mathcal{M} = -\sqrt{\frac{p_g \boldsymbol{\beta}_0^H \boldsymbol{L}^{-1} \boldsymbol{\beta}_0}{4}}, \tag{27}$$

and the dual optimization problem of $\mathcal{P}3$ can be constructed by

$$\mathcal{P}4: \quad \min_{\boldsymbol{\beta}_0} \quad \boldsymbol{\beta}_0^H \boldsymbol{L}^{-1} \boldsymbol{\beta}_0 \tag{28a}$$

$$\text{s.t.} \quad \boldsymbol{P} + \boldsymbol{N}\boldsymbol{\beta}_0 <= \mathbf{0}_{7\times 1} \tag{28b}$$

where $\boldsymbol{P}$= $\begin{bmatrix} \mathbf{0}_{4\times 1} \\ \mathbf{0}_{2\times 1} \\ 1 \end{bmatrix}$, $\boldsymbol{N}$= $\begin{bmatrix} -\boldsymbol{I}_{4\times 4} \\ -\boldsymbol{K_2}^T \\ -\boldsymbol{K_3}^T \boldsymbol{K_2}^T \end{bmatrix}$.

Based analysis and transformations above, we have simplified the original problem. Compared with $\mathcal{P}1$, $\mathcal{P}4$ can calculate the result more quickly and effectively by the gradient projection method [12], which is more conducive to practical application. The entire algorithm is summarized in Algorithm 1.

Algorithm 1 Efficient Algorithm to Solve $\mathcal{P}2$

Input: $s_{g,1}, s_{g,2}, \boldsymbol{h}_{g,1}, \boldsymbol{h}_{g,2}$
Output: $\boldsymbol{W}_g$, t

```
for b = 0.1 to 0.9 do
    Calculate λ̂ by P4 ;
    Get W_{g,b} by (16);
    Calculate P3;
    Get t_b.
end for
Choose b that maximizes R_{g,1} + R_{g,2};
Get t, W_g.
```

V. Simulation

In this section, we consider large-scale MU-MISO cells and use MATLAB software to simulate the proposed NOMA-CI precoding. We assume that the coverage area of the BS is within 300 meters, users in the cell are randomly and uniformly distributed. We define $K/8$ users with minimum channel gain as edge users, and according to the [13] set a reasonable number of users. The parameter settings for the simulation process are shown in Table I.

TABLE I
SIMULATION PARAMETER SETTINGS

Parameters	Parameter values
Transmitting power/W	P=[1, 9]
Number of users	K=[32, 128]
Total system bandwidth/MHz	10
Noise power spectral density/dBm/Hz	−174
Channel model	Rayleigh fading channel
Path loss factor	3

It can be seen from Fig. 5 that the system capacity obtained by NOMA-CI is better than the other two schemes when the system transmit power is $1w$, and the gap between NOMA-CI and CI tends to be obvious. Fig. 6(a) and 6(b) describe the vector graphs of user1 constructed by CI and NOMA-CI when two users transmit different symbolic information. It can be intuitively seen that NOMA-CI makes more useful work under the same power constraint. Fig. 6(c) and 6(d) describe the constructive precoding of user2 by the two schemes in this case. NOMA-CI directly eliminates the interference of other users and makes all power used for user2, making the signal quality obtained is better. As the number of users increases, the number of cases where two users have different symbolic information increases, so the gap between two precoding schemes is more pronounced. In addition, with the increase of users in the system, the total system capacity gradually decreases. This is because fewer users will provide more degrees of freedom to produce feasible precoding vectors when the number of transmitting antennas is fixed. Besides, the scheme under 8PSK has better system performance than that under QPSK. This is because spectrum utilization at 8PSK increases, allowing more information to be transmitted within the same bandwidth.

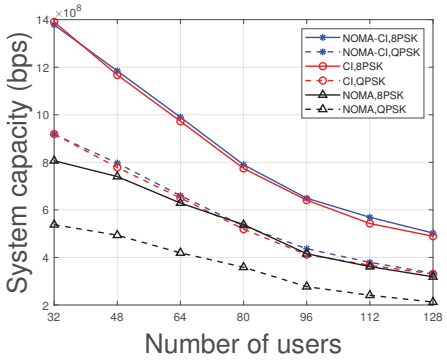

Fig. 5. System capacity versus number of users, N=128.

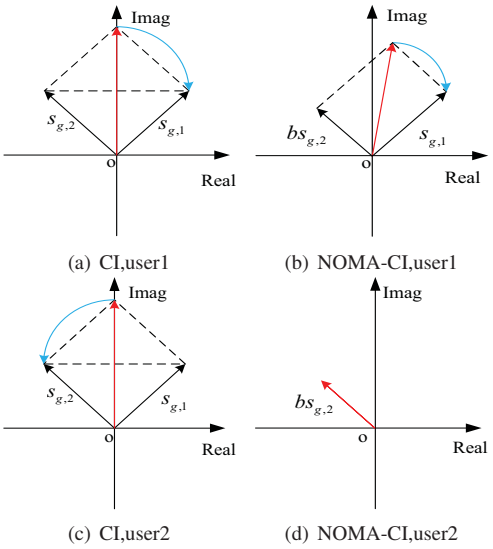

Fig. 6. Vector diagram of CI and NOMA-CI

Fig. 7 shows the changes in the system capacity of NOMA-CI precoding, traditional CI precoding and NOMA algorithm with the total transmission power of the system. Compared with the other two schemes, NOMA-CI has obvious advan-

tages under both QPSK and 8PSK constellations. NOMA-CI converts the intra-group interference in NOMA into constructive interference and improves the interference utilization efficiency of CI from a vector angle, greatly improving users' SNR. With the increase of transmission power, the SNR of users is greatly increased, and system capacity is also growing. However, as the transmission power increases, users are less affected by intra-group noise, so that the growth rate will slow down.

Fig. 8 describes the influence of different inter-group power distribution schemes on the capacity for edge users. It can be seen that the performance of our proposed proportional power distribution is better than the other two schemes. The average power distribution does not consider the difference in channel gain, and waterfilling distribution often allocates a larger power to users with good channel gain, both of which ignore the fairness between users.

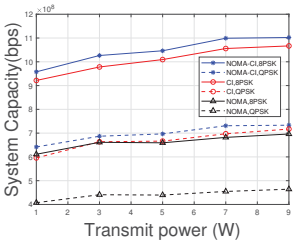

Fig. 7. System capacity versus transmit power, N=K=64.

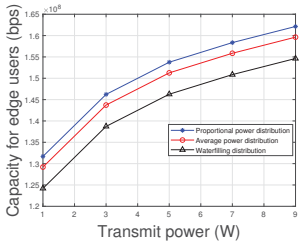

Fig. 8. Capacity for edge users under different power distribution methods, N=K=64.

As shown in Fig. 9 and Fig. 10, the capacity for edge users has the same trend as system capacity in two cases. The difference is that the capacity for edge users under NOMA-CI and CI is significantly higher than NOMA. This is because each user adopts SIC to decode useful information in a multi-user NOMA network, while the information of other users is treated as noise. The SNR of edge users will be significantly reduced due to the substantial discrepancy in channel gain between two users within each group. Through CI, the information of other users can be used to do useful work and the SNR of users with poor channel gain can be greatly improved. However, there is little difference between NOMA-CI and CI because they fully use of intra-group interference and both use large power to improve the capacity for edge users.

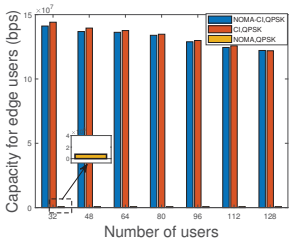

Fig. 9. Capacity for edge users versus number of users, N=128.

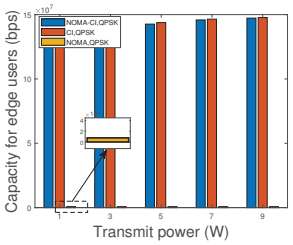

Fig. 10. Capacity for edge users versus transmit power, N=K=64.

VI. Conclusion

In this paper, considering the capacity for edge users, we employ a proportional power distribution scheme between groups. Then we design NOMA-CI precoding based on NOMA and CI, propose a max-min optimization problem and simplify the optimization problem using KKT and Lagrange. Simulation results show that the capacity for edge users is improved by proportional power distribution, and NOMA-CI precoding significantly improves system and edge user capacity. In the future, we will consider situations where CSI is inaccurate and investigate the performance of this precoding under quadrature amplitude modulation (QAM).

VII. Acknowledgement

This work was partly supported by the National Natural Science Foundation of China (Grants 62202035 and 61931001).

References

[1] P. V. Reddy, S. Reddy, S. Reddy, R. D. Sawale, P. Narendar, C. Duggineni, and H. B. Valiveti, "Analytical review on oma vs. noma and challenges implementing noma," in *2021 2nd International Conference on Smart Electronics and Communication (ICOSEC)*, 2021, pp. 552–556.

[2] J. Yu, X. Ning, Y. Sun, S. Wang, and Y. Wang, "Constructing a self-stabilizing cds with bounded diameter in wireless networks under sinr," in *IEEE INFOCOM 2017-IEEE Conference on Computer Communications*. IEEE, 2017, pp. 1–9.

[3] K. Chung, "Noma for correlated information sources in 5g systems," *IEEE Communications Letters*, vol. 25, no. 2, pp. 422–426, 2021.

[4] M. Atrouche, S. Ayad, and B. Mounir, "Comparative study of fairness and fixed power allocation algorithms : In non-orthogonal multiple access system," in *2022 7th International Conference on Image and Signal Processing and their Applications (ISPA)*, 2022, pp. 1–5.

[5] C. C. Chai and X.-P. Zhang, "Iterative water-filling power and subcarrier allocation for multicarrier non-orthogonal multiple access uplink," in *2022 IEEE International Symposium on Information Theory (ISIT)*, 2022, pp. 3043–3048.

[6] J. Dai, K. Niu, and J. Lin, "Iterative gaussian-approximated message passing receiver for mimo-scma system," *IEEE Journal of Selected Topics in Signal Processing*, vol. 13, no. 3, pp. 753–765, 2019.

[7] H. Al-Obiedollah, K. Cumanan, H. B. Salameh, G. Chen, Z. Ding, and O. A. Dobre, "Downlink multi-carrier noma with opportunistic bandwidth allocations," *IEEE Wireless Communications Letters*, vol. 10, no. 11, pp. 2426–2429, 2021.

[8] Z. Xiao, R. Liu, M. Li, Y. Liu, and Q. Liu, "Low-complexity designs of symbol-level precoding for mu-miso systems," *IEEE Transactions on Communications*, vol. 70, no. 7, pp. 4624–4639, 2022.

[9] M. Alodeh, S. Chatzinotas, and B. Ottersten, "Constructive multiuser interference in symbol level precoding for the miso downlink channel," *IEEE Transactions on Signal Processing*, vol. 63, no. 9, pp. 2239–2252, 2015.

[10] A. Salem, C. Masouros, and K.-K. Wong, "On the secrecy performance of interference exploitation with psk: A non-gaussian signaling analysis," *IEEE Transactions on Wireless Communications*, vol. 20, no. 11, pp. 7100–7117, 2021.

[11] A. M. Auyo, S. A. Babale, and L. M. Bello, "Effect of inspired cr-noma power allocation on bit error rate for three user noma system," in *2022 IEEE Nigeria 4th International Conference on Disruptive Technologies for Sustainable Development (NIGERCON)*, 2022, pp. 1–5.

[12] Q. Xu, P. Ren, and A. L. Swindlehurst, "Rethinking secure precoding via interference exploitation: A smart eavesdropper perspective," *IEEE Transactions on Information Forensics and Security*, vol. 16, pp. 585–600, 2021.

[13] S. Zarei, W. Gerstacker, and R. Schober, "Low-complexity widely-linear precoding for downlink large-scale mu-miso systems," *IEEE Communications Letters*, vol. 19, no. 4, pp. 665–668, 2015.